



**HAL**  
open science

## Mechanical properties of alumina-zirconia-Nb micro-nano hybrid composites

José F. Bartolomé, C.F. Gutiérrez-González, Ramón Torrecillas

► **To cite this version:**

José F. Bartolomé, C.F. Gutiérrez-González, Ramón Torrecillas. Mechanical properties of alumina-zirconia-Nb micro-nano hybrid composites. *Composites Science and Technology*, 2008, 10.1016/j.compscitech.2007.11.010 . hal-00499004

**HAL Id: hal-00499004**

**<https://hal.science/hal-00499004>**

Submitted on 9 Jul 2010

**HAL** is a multi-disciplinary open access archive for the deposit and dissemination of scientific research documents, whether they are published or not. The documents may come from teaching and research institutions in France or abroad, or from public or private research centers.

L'archive ouverte pluridisciplinaire **HAL**, est destinée au dépôt et à la diffusion de documents scientifiques de niveau recherche, publiés ou non, émanant des établissements d'enseignement et de recherche français ou étrangers, des laboratoires publics ou privés.

## Accepted Manuscript

Mechanical properties of alumina-zirconia-Nb micro-nano hybrid composites

José F. Bartolomé, C.F. Gutiérrez-González, Ramón Torrecillas

PII: S0266-3538(07)00465-4  
DOI: [10.1016/j.compscitech.2007.11.010](https://doi.org/10.1016/j.compscitech.2007.11.010)  
Reference: CSTE 3914

To appear in: *Composites Science and Technology*

Received Date: 14 June 2007  
Revised Date: 9 November 2007  
Accepted Date: 16 November 2007

Please cite this article as: Bartolomé, J.F., Gutiérrez-González, C.F., Torrecillas, R., Mechanical properties of alumina-zirconia-Nb micro-nano hybrid composites, *Composites Science and Technology* (2007), doi: [10.1016/j.compscitech.2007.11.010](https://doi.org/10.1016/j.compscitech.2007.11.010)

This is a PDF file of an unedited manuscript that has been accepted for publication. As a service to our customers we are providing this early version of the manuscript. The manuscript will undergo copyediting, typesetting, and review of the resulting proof before it is published in its final form. Please note that during the production process errors may be discovered which could affect the content, and all legal disclaimers that apply to the journal pertain.



# Mechanical properties of alumina-zirconia-Nb micro-nano hybrid composites

José F. Bartolomé<sup>1\*</sup>, C. F. Gutiérrez-González<sup>1</sup> and Ramón Torrecillas<sup>2</sup>

<sup>1</sup> Instituto de Ciencia de Materiales de Madrid, Consejo Superior de Investigaciones Científicas (CSIC), C/ Sor Juana Inés de la Cruz, 3, 28049 Madrid, Spain

<sup>2</sup> Instituto Nacional del Carbón, Consejo Superior de Investigaciones Científicas (CSIC), C/ Francisco Pintado Fe, 26, La Corredoira, 33010 Oviedo, Spain

## Abstract

The multi-scale and multi-phase hybrid composite ceramic-metal materials Al<sub>2</sub>O<sub>3</sub>-ZrO<sub>2</sub>-Nb are successfully fabricated. Their mechanical properties are better compared to the single-phase alumina materials and conventional alumina-Nb composite materials. The coexist function of nano-scale ZrO<sub>2</sub>, which can increase the initial toughness and strength, and the micrometer lamellar Nb particles which increase the toughness, flaw tolerance and crack growth resistance, improve notably the mechanical properties of these hybrid composites. The mechanisms of toughening and strengthening were analyzed, and it was found that residual stress, generated by the different thermal coefficients between the Al<sub>2</sub>O<sub>3</sub> matrix and the ZrO<sub>2</sub> nanoparticles, and bridging of the Nb inclusions were the two main factors that can increase the initial level of the driving force for critical microcrack extension, and shield an advancing crack and exert crack closure

stresses on the crack wake. The aim of this work is to develop mechanisms at a multiple of length scales in order to create a new hybrid material with unique mechanical properties.

Keywords: A. Ceramic-matrix composites; B. Toughness; B. Microstructure; Cermets

\* Author to whom all correspondence should be addressed.

E-mail addresses: jbartolo@icmm.csic.es

## Introduction

Advanced structural ceramics are regarded as attractive materials for many applications in industry, due to their wear resistance and excellent high-temperature properties. However, because of their low toughness and susceptibility to flaws, introduced either during processing or in service, industrial application has been limited. Over the past decades, the incorporation of fracture mechanics concepts into the design of ceramics had led to a marked increase in strength and toughness. The technique to develop even stronger materials through processing and microstructural refinements improves strength to an approximately equal extent throughout the range of starting flaw sizes, but still leaves the material with low toughness. On the other hand, there has been a focus on improving the inherent toughness of the ceramic through the control of the microstructural mechanisms [1]. In this regard, it is often useful to partition the mechanisms of fracture into “intrinsic” and “extrinsic” processes [2]. Intrinsic mechanisms evolve ahead of the crack tip (independent of crack size) while extrinsic mechanisms invariably evolve behind the crack tip (and dominate resistance-curve behavior). Such later mechanisms, which include crack bridging in composites, primarily “shield” locally the crack from the far-field (applied) “driving force”. One of the most

effective methods to incorporate these mechanisms is to introduce ductile metal secondary phases, like particles or fibres, in the ceramic matrix [3-6]. An important phenomenon associated with these toughening mechanisms in ceramic-metal composites is the increasing fracture resistance (increasing toughness) with crack extension (R-curve) [7-9]. Such an increase in fracture resistance provides damage tolerance characteristics to composites and narrows their strength distributions [10, 11]. This will typically improve the strength of the material for large initial flaws. However, these improvements are often achieved at the expense of strength for small flaws. The strength reduction can be dramatic, and since the naturally occurring flaws in a ceramic fall into this small flaw regime, the reduced strength can be a serious problem [12-15]. It is therefore pertinent to consider stress concentration around large defects, residual stresses and fracture initiation processes in these composites, and their subsequent influence on strength behaviour.

Experiments by many researchers [16, 17] have shown that the mechanical properties of a ceramic matrix can be significantly enhanced by the dispersion of second ceramic nanometer size particles to form a nanocomposite material. In these materials, the high strengths reported are not caused by an increase in toughness [18]. Several mechanisms have been proposed for enhancing the strength of nanocomposites; including thermal residual stresses, change in grain boundary morphology, dislocation activity, enhanced interfacial fracture energy, etc. However, a clear identification of the toughening mechanism in nanocomposites remains difficult because, first, the toughness increase is small or even absent and, second, there is no single persuasive mechanism. This suggests that nanocomposites may have limited structural use for engineering applications, at least where damage tolerance is required. Recently a new alumina/zirconia nanostructured ceramic with only 1.7 vol. % of nanoparticles of zirconia

with an average size of 150 nm have been fabricated [19]. These composites, due to the compressive residual stress developed, show fracture resistance properties never reached with oxide ceramics so far. These new composites, with toughening mechanisms operating on a scale smaller than the one of the matrix microstructure, can display a greater threshold for the stress intensity factor ( $K_{I0}$ ), under which crack propagation does not take place. On the other hand, these nanocomposites show flat R-curve behavior, and, therefore, damage tolerance is low [20].

While a large body of work focuses on the toughening effect of the ductile phase, little attention has been paid to the question of how strength and toughness are correlated [21-23]. Niihara [16] have shown that the hybridization of microcomposites and nanocomposites could result in a further improvement in both the strength and toughness. In the present study, we examine the fracture behavior of a new micro-nano hybrid composite,  $\text{Al}_2\text{O}_3\text{-ZrO}_2\text{-Nb}$ , where toughening and strengthening are achieved through the incorporation to  $\text{Al}_2\text{O}_3$  matrix of both Nb lamellar shape particles and  $\text{ZrO}_2$  nanoparticles. Niobium, being a refractory metal, was chosen due to its ductile constitutive behaviour and biocompatibility. Consequently, this particular family of composites can find applications in the field of biomaterials.

The aim of this paper is to consider mechanisms acting at the crack tip (i.e. at the nano-scale) and microstructural mechanisms occurring in the crack wake or at the crack front (i.e. at the micro-scale) to rationalize the approach of micro-nano hybrid composites. The knowledge of the respective influence of nano- and micro-scale mechanisms during crack initiation and propagation allows to define strategies for better crack growth resistance materials.

## Experimental

### Materials

Alumina nanopowders with 1.7 vol% (2,5 % wt.%) of  $ZrO_2$  were prepared from powder-alkoxide mixtures using  $\alpha$ -Alumina (99.99%) (TM-DAR, *Taimai Chemicals Co., LTD.*), with an average particle size of  $d_{50}=0.15 \mu m$ , a BET specific surface area of  $14.5 m^2/g$  and the following chemical analysis (ppm): Si (10), Fe (8), Na (8), K (3), Ca (3), Mg (2), Cu (1), Cr (<1), Mn (<1), U (<0.004), Th (<0.005) and zirconium IV-propoxide (70% solution in 1-propanol) (Sigma-Aldrich, Spain). In order to eliminate the humidity, alumina powder was first heated to  $250^\circ C$  during 10 hours. Stable slurry was prepared by dispersing alumina powder in anhydrous 99.97% ethanol. The sol was diluted in anhydrous 99.97% ethanol (66.7 vol% sol; 33.3 vol% anhydrous ethanol) and then added dropwise to the alumina slurry. After drying under magnetic stirring at  $70^\circ C$ , the powders were thermally treated at  $850^\circ C$  for 2 h in order to remove organic residuals and were subsequently attrition milled with alumina balls for 1 h. Further details on the powders preparation procedure are given in Schell et al [24].

Niobium powder (Goodfellow) of 99.85% purity and with an average particle size of  $d_{50}=35 \mu m$  was attrition milled with zirconia balls in a Teflon container during 4 h using Isopropilic alcohol as liquid media. Due to this process, niobium particles with a lamellar shape, high-aspect ratio and a  $d_{50}=41 \mu m$  were obtained.

Alumina- $nZrO_2$  and Alumina- $nZrO_2$  with 20 % vol. milled niobium suspensions of 80 wt% solid content were prepared using distilled water as liquid media and a 3 wt% addition of an alkali-free organic polyelectrolyte as surfactant. The mixtures were homogenized by milling with zirconia balls in polyethylene containers at 150 r.p.m. during 24 h and then dried at  $90^\circ C$  during 12 h. The resulting powders were ground in an

agate mortar and subsequently passed through a 75  $\mu\text{m}$  sieve. Finally, the powders were hot pressed at 1500  $^{\circ}\text{C}$  during 1 h with heating and cooling rates of 600  $^{\circ}\text{C}/\text{h}$  in an inert 100% Ar atmosphere. As a result, discs with 50 mm diameter and 5 mm thickness were obtained.

For comparison, an Alumina pure sample and alumina-20 vol% Nb composite were also prepared.

The  $\text{Al}_2\text{O}_3\text{-ZrO}_2$  nanopowder was characterized by transmission electron microscopy (TEM) using an electron microscopy, JEOL ARM model, operating a 1250 kV. The microstructure of sintered specimens was studied on surfaces polished down to 1  $\mu\text{m}$  by Scanning Electron Microscopy (SEM, Hitachi, model S3000N). The grain size of the alumina matrix was determined using linear intercept method. For the measurements of the  $\text{ZrO}_2$  grain size distribution, micrographs were taken of representative regions and the equivalent spherical diameters of 100 grains were measured.

#### Mechanical properties

The bending strength was determined using prismatic bars with 4 mm width, 45 mm length and 3 mm thickness by three-point bending test. The tensile surface of the bars was polished down to 1  $\mu\text{m}$ . The tests were performed at room temperature using a universal testing machine (Instron Model 4411, Boston, MA) and were conducted in loading direction perpendicular to the lamellar Nb particles. The specimens were loaded to failure with a cross-head speed of 0.5 mm/min and a span of 40 mm. Young's modulus was obtained from the slopes of load-deflection curves of three-point bending test. The damage tolerance of the specimens was measured by analyzing the strength data for specimens as a function of indentation load (i.e. indentation-strength test). Reported

strengths represented the mean and standard deviation of at least 20 specimens. The main advantages of this method are the relative simplicity, small specimen size required, and the fact that the indentation-induced cracks are similar to the “natural” flaws pre-existing in the material in both shape and dimension. The centres of the tensile faces of the bars were indented with a Vickers diamond indenter (leco 100-A, St. Joseph, MI) at contact loads between 10 and 500 N. Special effort was made to examine all specimens after testing using reflected light optical microscopy (Leica, Model DMR), to verify that the indentation contact sited acted as the origin of failure. The hardness was estimated by the Vickers indentation.

The indentation-strength technique has been also employed to evaluate the R-curve behaviour [25]. The fracture toughness of the composites was examined by measuring the resistance-curve in terms of the stress intensity required for crack initiation and subsequent growth as a function of crack extension. A family of global stress intensity stress versus crack sizes curves at each indentation load and its corresponding strength are plotted. An envelope of tangency points is fitted to these curves to yield the R-curve. This technique has been widely used in studying the crack growth resistance behaviour of composites and nanocomposites [26-30].

After testing, profiles of cracks paths and fracture surfaces were examined using scanning electron microscopy.

## Results

### Microstructural analysis and mechanical properties

A representative TEM image of  $\text{Al}_2\text{O}_3$ - $\text{ZrO}_2$  nanopowder is shown in Fig. 1. As can be seen, zirconia nanocrystals (~ 10 nm diameter) sit on the surface of the  $\text{Al}_2\text{O}_3$

particles. Figure 2 show SEM images of a thermally etched, polished section of monolithic  $\text{Al}_2\text{O}_3$ ,  $\text{Al}_2\text{O}_3$ - $\text{ZrO}_2$  composites. The  $\text{ZrO}_2$  and  $\text{Al}_2\text{O}_3$  grains are the brighter and darker phase respectively. The composite show nano-sized  $\text{ZrO}_2$  particles homogeneously distributed. Those zirconia particles are found to be intergranular ( $D_{50} \approx 90$  nm), situated at either grain boundaries or triple points (Fig. 2b). The alumina grains ( $D_{50} \approx 0.5$   $\mu\text{m}$ ) are equiaxial and exhibit a relatively broad grain size distribution. The addition of a second  $\text{ZrO}_2$  nanophase impedes the grain growth by a pinning effect, i.e., the grain growth of the matrix was much reduced compared to the monolithic system due to the blocking of alumina growth by the zirconia grains. The pure alumina had a mean particle size of 2.5  $\mu\text{m}$ .

The bending strength, Young's modulus and hardness for the studied specimens are given in Table 1.

#### Damage tolerance

Figure 3 presents the indentation strength as a function of the indentation load. For the monolithic alumina and  $\text{Al}_2\text{O}_3$ - $\text{ZrO}_2$  composite the slopes, obtained by the linear regression method, were -0.25 and -0.27 respectively, which implies that the fracture toughness changed little with crack growth. However, for the  $\text{Al}_2\text{O}_3$ - $\text{ZrO}_2$ -Nb and  $\text{Al}_2\text{O}_3$ -Nb composites, the slopes were -0.15 and -0.16 respectively. The low absolute value for the slope indicates that the strength reduction by indentation cracks is smaller and that fracture toughness increases slowly with increasing crack length. Figure 3 shows that whereas indentations at 10 N do not degrade the ensuing strength properties in micro-nano hybrid composite, the same indentations cause substantial loss of strength in nanocomposites and alumina materials.

## Fracture toughness and R-curve behavior

The R-curve behavior of the  $\text{Al}_2\text{O}_3\text{-ZrO}_2\text{n-Nb}$  composites is shown in Fig. 4 and clearly illustrates the significantly higher fracture resistance of the ceramic-metal composites compared to unreinforced  $\text{Al}_2\text{O}_3\text{-ZrO}_2\text{n}$  composite and monolithic  $\text{Al}_2\text{O}_3$ . For the  $\text{Al}_2\text{O}_3\text{-ZrO}_2\text{n-Nb}$  composite, cracking initiated at  $\sim 6 \text{ MPa}\cdot\text{m}^{1/2}$ , and involved stable crack advanced at progressively higher stress intensities exceeding  $12 \text{ MPa}\cdot\text{m}^{1/2}$  due to crack bridging by intact Nb lamellar particles in the crack wake. In contrast, the  $\text{Al}_2\text{O}_3\text{-ZrO}_2\text{n}$  material and monolithic  $\text{Al}_2\text{O}_3$  failed catastrophically at  $K_{\text{IC}}$  values of 6 and 4.5 respectively. For these materials, the fracture toughness rose rapidly at the relatively short crack length and did not increase much thereafter. The rapid rise of the fracture toughness should be caused by the relatively small grain sizes in these materials. On the other hand, the  $\text{Al}_2\text{O}_3\text{-Nb}$  composite showed a lower R-curve behavior than the  $\text{Al}_2\text{O}_3\text{-ZrO}_2\text{n-Nb}$  composite. Initially, fracture toughness was similar to the monolithic alumina, but with growing crack, fracture toughness increased, reaching over  $10 \text{ MPa}\cdot\text{m}^{1/2}$  when the crack was longer than  $\sim 700 \mu\text{m}$ .

Crack extension commences at crack-tip stress intensity for crack initiation,  $K_{\text{t}}$ , while sustaining further crack extension requires higher driving forces until typically a “plateau” or steady-state toughness is reached. Two points are noteworthy. First, the comparison between the  $\text{Al}_2\text{O}_3\text{-ZrO}_2\text{n}$  composite and the monolithic  $\text{Al}_2\text{O}_3$  demonstrates the ability of nanoparticles to impart toughening mechanisms operating on a scale smaller than the one of the matrix microstructure, enhancing the “intrinsic” fracture properties of the material [20]. Secondly, it appears that lamellar metal reinforcements in  $\text{Al}_2\text{O}_3\text{-Nb}$  and  $\text{Al}_2\text{O}_3\text{-ZrO}_2\text{n-Nb}$  composites are effective in enhancing the fracture resistance with

the crack propagation, showing stable crack-growth resistance behaviour (R-curve). Quantitatively, the magnitude of such toughening can be modeled in terms of the increase in the strain energy release rate from tractions produced by the intact Nb ligaments bridging the two crack surfaces. In the present case, where the length of the bridging zone is small compared to the specimen dimensions (small scale bridging), the fracture toughness increase with crack extension up to a maximum steady-state level,  $K_{ss}$ , can be estimated in terms of the volume fraction,  $f$ , yield strength,  $\sigma_y$ , and a representative cross-sectional radius,  $t$ , of the reinforcement as [31]:

$$\Delta K_{ss} = \sqrt{K_t^2 + Eft\sigma_y\chi} \quad (1)$$

where  $E$  is the Young's modulus of the composite and  $\chi$  a dimensionless function representing the work of rupture. Taking the volume fraction of ductile Nb phase intercepted by the crack path as  $f \sim 0.12$ , assuming that over 60 % of particles were found to fail with some degree of deformation, and using  $\sigma_y$  for Nb  $\sim 170$  MPa [32],  $E \sim 340$  GPa,  $t \sim 3 \mu\text{m}$  (half lamellar particle thickness) and  $\chi \sim 2.5$  (assuming a well bonded interface) [33] the predicted steady-state toughness of  $\sim 12 \text{ MPa}\cdot\text{m}^{1/2}$  is obtained, which is in fair agreement with the experimental result.

#### Crack/particle interactions

Scanning electron micrographs of fracture surfaces confirm that the higher toughness in the present  $\text{Al}_2\text{O}_3\text{-ZrO}_2\text{-Nb}$  composite can be attributed to the crack bridging of the metal particles. A typical fracture surface of a bend bar at room temperature is depicted in Fig. 5. The ceramic matrix exhibits intergranular fracture, whereas the reinforcing Nb particles display features of both ductile and brittle fracture. It should be noted, that cleavage fracture in body-centered cubic materials, such as Nb, is

promoted by triaxial constraint which acts to restrict plastic stretching of the metal [34]. Interstitial impurities (most likely oxygen in this case) and the large grain size of the Nb rounded particles may also be contributing factors. Where the Nb particles fail by a combination of both mechanisms, the fracture surfaces show regions of void coalescence separating cleavage facets that penetrate into and out of the crack plane.

## Discussion

Many applications require not only high strength, but also high toughness. In terms of microstructural design, requirements for high strength are often different or even contradictory to those for high fracture toughness. For example, fine equiaxed grained alumina improves strength, but decreases toughness due to the lack of crack bridging. On the other hand, large grained alumina improves toughness and flaw tolerance, but results in low strength. Some researches suggested the compromise must be made between these requirements. One sacrifices strength to gain some flaw tolerance, or one improves strength at the expense of some flaw tolerance or toughness. [35] Thus, for any given ceramic material, strength and toughness tend to have an inverse relationship [36]. Considering toughness first, ceramics generally exhibit R-curve behavior with enhancement of long-crack toughness relative to short-crack toughness at larger grain sizes. Whereas short-crack toughness is governed by intrinsic grain boundary or interfaces energies, long-crack toughness is augmented by dissipative crack-tip shielding processes, such as bridging. The strength of most materials, especially brittle ceramics, is determined by their resistance to both the initiation of cracks from defects and their subsequent propagation. In the  $\text{Al}_2\text{O}_3$ -Nb composite, the addition of metal inclusions significantly decreases the strength of these composites (Table 1). Though the strength

may be sacrificed slightly by adopting this approach, the reinforcement also acts as stress concentration site. However, this method is attractive as the reliability of ceramics during the subsequent usage can be significantly improved. Therefore, an important limitation associated with grain bridging involves the length scales over which it operates. In order to develop a saturated bridging zone, the peak (or long-crack) fracture toughness is not reached until cracks are substantially above microstructural dimensions. This scaling effect gives rise to the ubiquitous “resistance-curve”. Because the saturation distance (or bridging zone length) is typically on the order of  $\sim 700 \mu\text{m}$ , long crack toughness do not apply to microstructurally small cracks. Therefore, the R-curve plateau toughness is not necessarily critical for the strength of metal-reinforced ceramics, more likely being the initial toughness which determines strength.

Previous studies [37, 38] on the R-curve behaviour in ceramics established by crack growth of indentation cracks in controlled bending tests, have shown that a threshold crack resistance exists. When applied stress intensity is smaller than such threshold stress intensity, no stable crack growth may be observed. For  $\text{Al}_2\text{O}_3\text{-ZrO}_2\text{-Nb}$  composites, the increase of intrinsic toughness can impart a high resistance to crack initiation, and therefore can be strengthened the material. Here the concept of tailoring strength by inhibition of crack initiation makes use of the heterogeneous thermo-elastic properties of the micro-nano hybrid composite phases. Due to thermal expansion misfit, the ceramic matrix is set under compressive residual stresses [39]. Therefore, the critical applied tensile stress for crack initiation is shifted to a higher level. On the other hand, the internal compressive stress acting on the alumina/alumina interfaces due to the intergranular located zirconia nanoparticles, enhances the formation of a strong boundary structure decreasing the total probability of intergranular fracture. Consequently, the

tensile residual microstresses expected at some grain boundaries of polycrystalline alumina, due to thermoelastic anisotropy, were reduced. As a result, the use of the shortest crack growth threshold, the minimum driving force for any crack extension, is a useful design criterion for bridging ceramic composites with R-curve behavior.

The current results demonstrate that nanocomposite and ductile phase toughening concepts can be successfully utilized together to enhance the intrinsic fracture toughness and crack growth resistance of ceramic materials. In this concept, the strong grain boundary, due to the presence of intergranular nanoparticles, can impart a high resistance to crack initiation, whereas the elongated ductile grains can enhance the crack growth resistance (R-curve) and flaw tolerance. Opportunities for the next generation of multi-phase and multi-scale hybrid ceramics lie with microstructural designed ceramics. From our study, we foresee a tremendous potential for the microstructural design at different scales of composites to change the very nature of the damage behavior and therefore to optimize the mechanical response to suit particular applications.

## Conclusions

Based on a study of the fracture toughness and resistance curve behavior of ductile Nb reinforced  $\text{Al}_2\text{O}_3\text{-ZrO}_2$  nanocomposites, the following conclusions can be made:

- The incorporation of just 1.7 vol% of  $\text{ZrO}_2$  nanoparticles significantly improved the average bend strength of monolithic alumina (~520 MPa) to 630 MPa. Simultaneously, the fracture toughness was increased from 4 to 6  $\text{MPa}\cdot\text{m}^{1/2}$ .

- Effective resistance-curve toughening of  $\text{Al}_2\text{O}_3\text{-ZrO}_2$  was achieved through reinforcement with lamellar shape Nb particles. With only 20 vol%, the toughness of  $\text{Al}_2\text{O}_3\text{-ZrO}_2$  was increased from 6 to 14  $\text{MPam}^{1/2}$ .
- The design of micro/nano hybrid composite opens the possibility to tailor new materials with toughening mechanisms operating at different scales. For a scale below the one of the matrix microstructure, this enhances the “intrinsic” fracture properties of the material. This intrinsic increase of resistance to crack initiation and propagation due to a structural synergism between the matrix phase and dispersoid, should lead to an increase in the catastrophic failure strength. On the other hand, the extrinsic mechanism like bridging of the ductile metallic elongated particles can enhance the crack growth resistance (R-curve) and flaw tolerance. In other words, in this case strength and toughness increases are compatible.

### **Acknowledgements**

This work was supported by EU under the project reference FP6-515784-2, by the Spanish Ministry of Science and Technology under the project number MAT2006-10249-C02-01, and by the “Dirección General de Universidades e Investigación de la Consejería de Educación y Ciencia de la Comunidad de Madrid” and CSIC under the project reference 200660M042. J.F.B. has been supported by Ministry of Science and Technology and CSIC by the “Ramón y Cajal” Program, co-financed by the European Social Fund.

## REFERENCES

- 1 Evans AG. Perspective on the development of high-toughness ceramics. *J. Am. Ceram. Soc.* 1990;73(2):187-206.
- 2 Ritchie RO, Gilbert CJ, McNaney JM. Mechanics and mechanisms of fatigue damage and crack growth in advanced materials. *Int. J. Solids Struct.* 2000;37(1-2):311-329.
- 3 Bartolome JF, Diaz M, Requena J, Moya JS. Mullite/molybdenum ceramic-metal composites. *Acta Mater.* 1999;47(14):3891-3899.
- 4 Flinn BD, Ruhle M, Evans AG. Toughening in composites of  $\text{Al}_2\text{O}_3$  reinforced with Al. *Acta Metall. Mater.* 1989;37(11):3001-3006.
- 5 Sigl LS, Mataga PA, Dalgleish BJ, McMeeking RM, Evans AG. On the toughness of brittle materials reinforced with a ductile phase. *Acta Metall. Mater.* 1988;36(4):945-953.
- 6 Zimmermann A, Hoffman M, Emmel T, Gross D, Rödel J. Failure of metal-ceramic composites with spherical inclusions. *Acta Mater.* 2001;49(16):3177-3187.
- 7 Nagendra N, Jayaram V. Fracture and R-curves in high volume fraction  $\text{Al}_2\text{O}_3/\text{Al}$  composites. *J. Mater. Res.* 2000;15(5):1131-1144.
- 8 Raddatz O, Schneider GA, Mackens W, Vob H, Claussen N. Bridging stresses and R-curves in ceramic/metal composites. *J. Eur. Ceram. Soc.* 2000;20(13):2261-2273.
- 9 Sbaizero O, Pezzotti G, Nishida T. Fracture energy and R-curve behavior of  $\text{Al}_2\text{O}_3/\text{Mo}$  composites. *Acta Mater.* 1998;46(2):681-687.

- 10 Bartolome JF, Requena J, Moya JS, Li M, Guiu F. Cyclic fatigue crack growth resistance of  $\text{Al}_2\text{O}_3$ - $\text{Al}_2\text{TiO}_5$  composites. *Acta Mater.* 1996;44(4):1361-1370.
- 11 Cook RF, Clarke DR. Fracture stability, R-curves and strength variability. *Acta Metall. Mater.* 1988;36(3):555-562.
- 12 Dutta AK, Narasaiah N, Chattopadhyaya AB, Ray KK. The load dependence of hardness in alumina-silver composites. *Ceram. Int.* 2001;27(4):407-413.
- 13 Rodeghiero ED, Tse OK, Chisaki J, Giannelis EP. Synthesis and properties of Ni-Alpha- $\text{Al}_2\text{O}_3$  composites via sol-gel. *Mat. Sci. Eng. A-Struct.* 1995;195(1-2):151-161.
- 14 Tuan WH, Chen WR. Mechanical-properties of alumina-zirconia-silver composites. *J. Am. Ceram. Soc.* 1995;78(2):465-469.
- 15 Vekinis G, Sofianopoulos E, Tomlinson WJ. Alumina toughened with short nickel fibres. *Acta Mater.* 1997;45(11):4651-4661.
- 16 Niihara K. New design concept of structural ceramics. *Ceramic nanocomposites J. Ceram. Soc. Jpn.* 1991;99(10):974 - 982.
- 17 Sternitzke M. Structural ceramic nanocomposites. *J. Eur. Ceram. Soc.* 1997;17(9):1061-1082.
- 18 Derby B. Ceramic nanocomposites: mechanical properties. *Current Opinion in Solid State Mat. Sci.* 1998;3(5):490-495.
- 19 Chevalier J, Deville S, Fantozzi G, Bartolomé JF, Pecharromán C, Moya JS.. Nanostructured ceramic oxides with a slow crack growth resistance close to covalent materials. *Nano Lett.* 2005;5(7):1297-1301.
- 20 J. Chevalier, S. Deville, G. Fantozzi, J. F. Bartolomé, C. Pecharroman, J. S. Moya, and R. Torrecillas “Advanced Nanocomposite Materials for Orthopaedic

- Applications. II. Reliability assessment” *Journal of Biomedical Materials Research Part B: Applied Biomaterials*, In Press
- 21 Bannister M, Shercliff H, Bao G, Zok F, Ashby MF. Toughening in brittle systems by ductile bridging ligaments. *Acta Metall. Mater.* 1992;40(7):1531-1537.
- 22 Bao G, Zok F. On the strength of ductile particle-reinforced brittle-matrix composites. *Acta Metall. Mater.* 1993;41(12):3515-3524.
- 23 Prielipp H, Knechtel M, Claussen N, Streiffer S, Müllejans H. Rüle M, Rödel J. Strength and fracture-toughness of aluminum alumina composites with interpenetrating networks. *Mat. Sci. Eng. A-Struct.* 1995;197(1):19-30.
- 24 Schehl M, Diaz LA, Torrecillas R. Alumina nanocomposites from powder-alkoxide mixtures. *Acta Mater.* 2002;50(5):1125-1139.
- 25 Braun LM, Bennison SJ, Lawn BR. Objective evaluation of short-crack toughness curves using indentation flaws - case-study on alumina-based ceramics. *J. Am. Ceram. Soc.* 1992;75(11):3049-3057.
- 26 Bartolome JF, Diaz M, Moya JS. Influence of the metal particle size on the crack growth resistance in mullite-molybdenum composites. *J. Am. Ceram. Soc.* 2002;85(11):2778-2784.
- 27 Khan A, Chan HM, Harmer MP. Toughness-curve behavior of an alumina-mullite composite. *J. Am. Ceram. Soc.* 1998;81(10):2613-2623.
- 28 Lawn BR, Padture NP, Braun LM, Bennison SJ. Model for toughness curves in 2-phase ceramics .I. Basic Fracture-Mechanics. *J. Am. Ceram. Soc.* 1993;76(9):2235-2240.

- 29 Rodriguez-Suarez T, Lopez-Esteban S, Bartolome JF, Moya JS. Mechanical properties of alumina-rich magnesium aluminate spinel/tungsten composites. *J. Eur. Ceram. Soc.* 2007;27(11):3339-3344.
- 30 Yang JF, Sekino T, Choa YH, Niihara K, Ohji T. Microstructure and mechanical properties of sinter-post-HIPed  $\text{Si}_3\text{N}_4$ -SiC composites. *J. Am. Ceram. Soc.* 2001;84(2):406-412.
- 31 Bencher CD, Sakaida A, Venkateswara Rao KT and Ritchie RO. Toughening mechanisms in ductile niobium-reinforced niobium aluminide ( $\text{Nb}/\text{Nb}_3\text{Al}$ ) in situ composites. *Metall. Mater. Trans.* 1995;26A(8):1995-2027.
- 32 Cardarelli F. *Materials Handbook*. London: Springer, Verlag, 2000.
- 33 Deve HE, Evans AG, Odette GR, Mehrabian R, Emiliani ML Hecht RJ. Ductile reinforcement toughening of gamma-TiAl - effects of debonding and ductility. *Acta Metall. Mater.* 1990;38(8):1491-1502.
- 34 Kajuch J, Short J, Lewandowski JJ. Deformation and fracture-behavior of Nb in  $\text{Nb}_5\text{Si}_3/\text{Nb}$  laminates and its effect on laminate toughness. *Acta Metall. Mater.* 1995;43(5):1955-1967.
- 35 Bennison SJ, Padture NP, Runyan JL, Lawn BR. Flaw-insensitive ceramics. *Phil. Mag. Lett.* 1991;64(4):191-195.
- 36 Lawn BR. *Fracture of Brittle Solids*. Cambridge: Cambridge University Press, 1993.
- 37 Gong JH, Guan ZD. Characterization of R-curve behavior in  $\text{Si}_3\text{N}_4$ -based ceramics. *Mat. Sci. Eng. A-Struct.* 2001;318(1-2):42-49.

- 38 Lube T, Fett T. A threshold stress intensity factor at the onset of stable crack extension of Knoop indentation cracks. *Eng. Fract. Mech.* 2004;71(16-17):2263-2269.
- 39 Bartolome JF, De Aza AH, Martin A, Pastor JY, Llorca J, Torrecillas R, Bruno G. alumina/zirconia micro/nanocomposites, a new material for biomedical applications with superior sliding wear resistance. *J. Am. Ceram. Soc.* 2007; 90(10) 3177-3184.

ACCEPTED MANUSCRIPT

Table 1.

<b>SAMPLE</b>	<b><math>\sigma_f</math> (MPa)</b>	<b>YOUNG'S MODULUS (GPa)</b>	<b>HARDNESS (GPa)</b>
<b>Al<sub>2</sub>O<sub>3</sub></b>	520±13	360±4	20±0.2
<b>Al<sub>2</sub>O<sub>3</sub>-Nb</b>	400±11	345±5	13.6±0.5
<b>Al<sub>2</sub>O<sub>3</sub>-2.5ZrO<sub>2</sub></b>	630±18	380±5	23.4±0.9
<b>Al<sub>2</sub>O<sub>3</sub>-2.5ZrO<sub>2</sub>-Nb</b>	600±10	340±4	14.5±0.5

ACCEPTED MANUSCRIPT

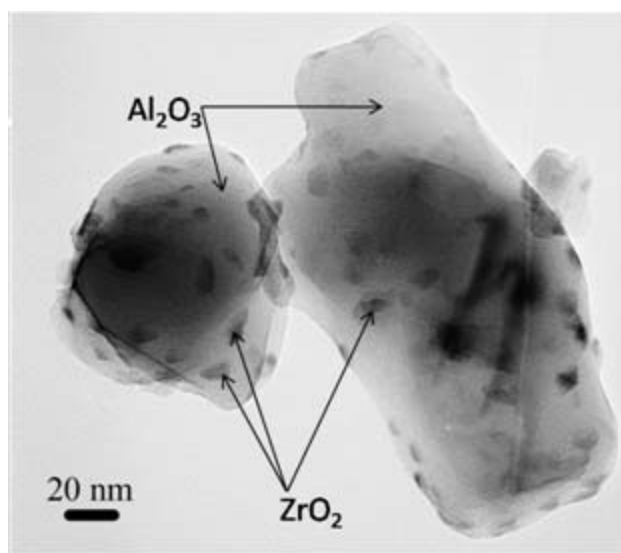


Fig. 1. TEM image of  $\text{Al}_2\text{O}_3$ - $\text{ZrO}_2$  nanopowder.

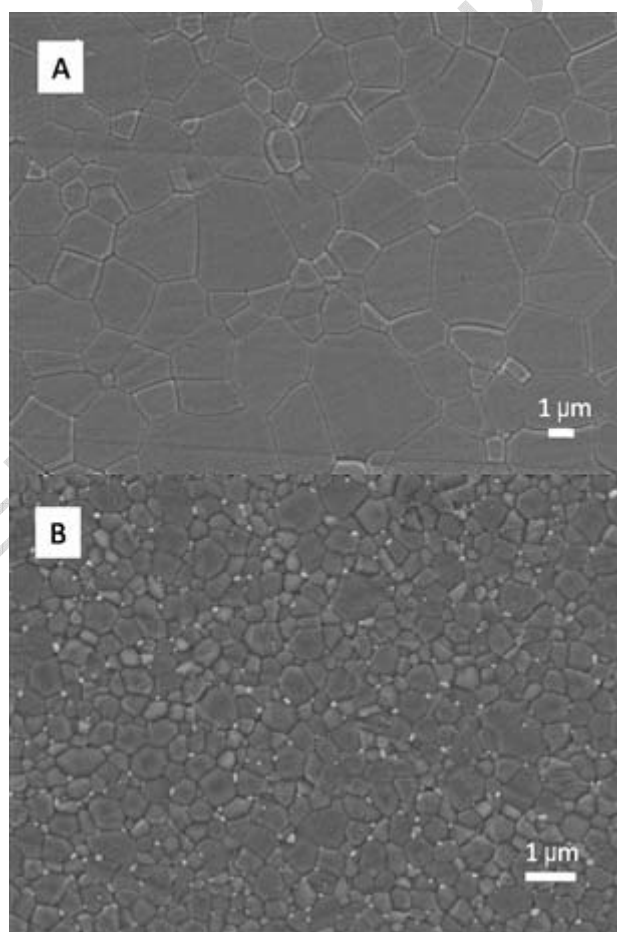


Fig.2. SEM images of a thermally etched, polished section of monolithic  $\text{Al}_2\text{O}_3$  (A) and  $\text{Al}_2\text{O}_3$ - $\text{ZrO}_2$  composites (B).

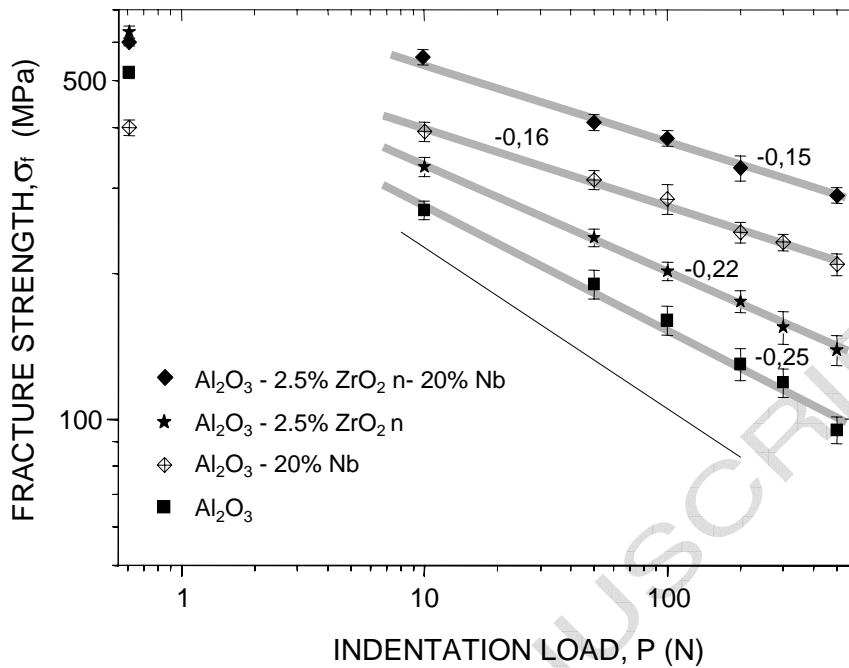


Fig.3. Indentation load versus strength plots of the different materials. The indentation-strength data to the  $P^{-1/3}$  strength response is shown by the diagonal dashed line.

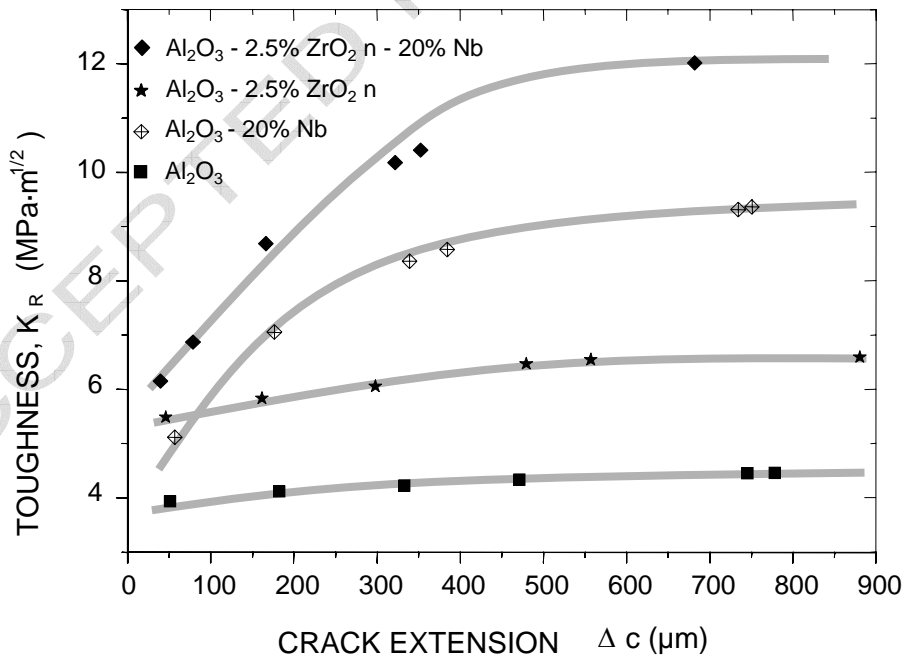


Fig.4. Comparison of the R-curves measured in all the materials.

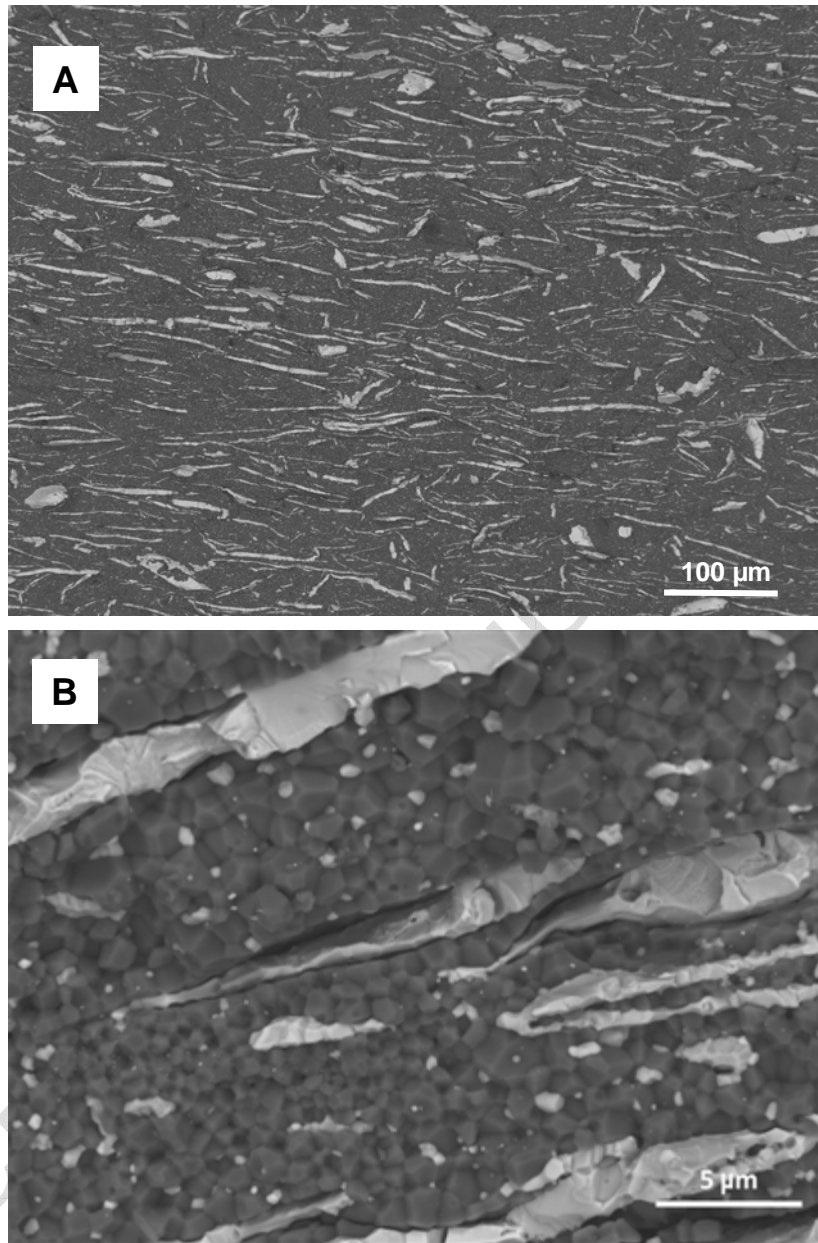


Fig. 5. A typical fracture surface of a bend bar tested at room temperature of the  $\text{Al}_2\text{O}_3$ - $\text{ZrO}_2$ - $\text{Nb}$  composite. (A) General view and (B) close-up where the inclusion fails can be noticed. Micrograph show apparent cleavage fracture and intact ductile bridging ligaments, which dissipate plastic energy by necking and shear banding during failure.